PAPER

In situ X-ray reflectivity studies of molecular and molecular-cluster intercalation within purple membrane films

Noor Haida Mohd Kaus,[af] Andrew M. Collins,[*b] Oier Bikondoa,[cd] Philip T. Cresswell,[e] Jennifer M. Bulpett,[e] Wuge H. Briscoe[*e] and Stephen Mann[ef]

It has been recently demonstrated that molecular and molecular cluster guest species can intercalate within lamellar stacks of purple membrane (PM), and be subsequently dried to produce functional bioinorganic nanocomposite films. However, the mechanism for the intercalation process remains to be fully understood. Here we employ surface X-ray scattering to study the intercalation of aminopropyl silicic acid (APS) or aminopropyl-functionalised magnesium phyllosilicate (AMP) molecular clusters into PM films. The composite films are prepared under aqueous conditions by guest infiltration into preformed PM films, or by co-assembly from an aqueous dispersion of PM sheets and guest molecules/clusters. Our results show that addition of an aqueous solution of guest molecules to a dried preformed PM film results in loss of the lamellar phase, and that subsequent air-drying induces re-stacking of the lipid/protein membrane sheets along with retention of a 2–3 nm hydration layer within the inter-lamellar spaces. We propose that this hydration layer is necessary for the intercalation of APS molecules or AMP oligomers into the PM film, and their subsequent condensation and retention as nano-thin inorganic lamellae within the composite mesostructure after drying. Our results indicate that the intercalated nanocomposites prepared from preformed PM films have a higher degree of ordering than those produced by co-assembly.

Introduction

Intact sheets of purple membrane (PM), consisting of hexagonally packed trimeric arrays of the protein bacteriorhodopsin (*bR*) embedded within a lipid bilayer membrane 4.7 nm in thickness, can be readily isolated from the organism *Halobacterium salinarium*. PM sheets are typically 500–1000 nm in size, and of technological importance due to the photochromic and light harvesting properties of *bR*, which can pump protons from the cytoplasmic to extracellular side of the membrane under illumination.[1] These properties have led to the development of novel PM-based materials for holography, photoswitching and memory storage applications.[2,3] The photocycle in PM is well understood, with established structural and temporal models describing the process of proton shuttling through the membrane with angstrom and femtosecond resolution.[4,5] In this process, water provides the main source of proton donation to *bR*, and so the behaviour and interaction of water molecules near the surface of the PM sheets is of particular mechanistic interest.[6–9]

In many technical applications, PM sheets are stacked by controlled sedimentation into mesostructured thin films that require some level of hydration to retain their proton-pumping functionality.[10,11] Hybrid films formed by intercalating a guest material with the PM sheets are more structurally robust than pure PM films,[12] but intercalation can impact on protein functionality due to inhibition of water transport through the film. Therefore, understanding the mechanism of intercalation and the role of hydration in the intercalation process and resultant film functionality are important aspects for the design and construction of hybrid PM films.

Previous structural studies on PM thin films using neutron reflectivity (NR) and X-ray reflectivity (XRR) have focused on the role of water that exists in the films after their formation. It has been shown that PM films exhibit a lamellar structure with an interlayer spacing of 4.7 nm when prepared at less than 10% relative humidity (RH), which swells to 6.2–8.0 nm at RH > 95%.[13,14] The swelling in the lamellar spacing is attributed to

a School of Chemical Sciences, Universiti Sains Malaysia, 11800, Penang, Malaysia

b Bristol Centre for Functional Nanomaterials, Centre for Nanoscience and Quantum Information, University of Bristol, Bristol, UK, BS8 1FD. E-mail: andy.collins@bristol.ac.uk

c XMaS, The UK-CRG Beamline at the ESRF, The European Synchrotron, CS 40220, 38043 Grenoble CEDEX 9, France

d Department of Physics, University of Warwick, Gibbet Hill Road, Coventry, CV4 7AL, UK

e School of Chemistry, University of Bristol, Cantock's Close, Bristol BS8 1TS, UK. E-mail: wuge.briscoe@bristol.ac.uk

f Centre for Organized Matter Chemistry, School of Chemistry, University of Bristol, Cantock's Close, Bristol BS8 1TS, UK

This journal is © The Royal Society of Chemistry 2014

J. Mater. Chem. C, 2014, **2**, 5447–5452 | 5447

interstitial water molecules, which were found to exhibit retarded rotational motion and reduced translational diffusion in the direction of stacking compared to the bulk free liquid. The role of water within the films has been described as analogous to a lubricant, allowing for the necessary conformational changes in *bR* during illumination as well as providing a source of protons for the photocycle.[13] This has been confirmed by XRR studies on the thermal decomposition of fully dehydrated PM films, which maintained protein functionality after exposure to temperatures as high as 140 °C.[15] In a water-free lamellar PM stack there was a reduction in allowable conformal motion available to *bR*, which inhibited denaturation. Under dehydration it was found that the *bR* assemblies rigidified and became locked in their 2D short range structure, resulting in a corrugation of the PM sheet, as observed by diffuse scattering. The corrugation disappeared when the film was swollen with interdigitated water, indicating that flexibility was restored to the PM sheet.[15]

Hydration also plays an important role in the formation of intercalated PM films hosting guest molecules and materials. It has been shown that hybrid films consisting of PM sheets intercalated with a condensed organosilane can be formed by adding an aqueous precursor to a PM lamellar film and then allowing the samples to dry.[12,16,17] These composite films demonstrate enhanced mechanical tolerance and solvent resistance in addition to functional photocycle and photochromic responses. Importantly, the composite films retain their lamellar structure as opposed to dispersal of the PM sheets randomly within an organic or inorganic supporting matrix. Critically, it was not known from these studies whether the hydrolysed organosilane precursors coated the PM sheets in suspension prior to reassembly and condensation, or the guest species permeated into the assembled film as the concentration increased upon drying. Intercalation in PM films of non-sol–gel precursors such as polysaccharides, inorganic polymers and polycationic organoclay oligomers has also been demonstrated, but the mechanism by which the guest materials permeated into the PM host structure was not fully elucidated.[16,18]

In this paper we have used X-ray surface scattering to study the mechanism of formation of PM films intercalated with aminopropyl silicic acid (APS) or cationic oligomers of aminopropyl-functionalised magnesium phyllosilicate (AMP), as two model guest species presented in molecular or molecular-cluster forms, respectively. Both of these guests have been previously used to produce PM-based composite films with an AB-type lamellar structure.[16] The composite films are prepared under aqueous conditions by guest infiltration into preformed PM films, or by co-assembly from an aqueous dispersion of PM sheets and guest molecules/clusters. Our results show that addition of an aqueous solution of guest molecules to a dried preformed PM film results in loss of the lamellar phase, and that subsequent air-drying induces re-stacking of the lipid/protein membranes along with retention of a 2–3 nm hydration layer within the inter-lamellar spaces. We propose that this hydration layer is necessary for the intercalation of APS molecules or AMP oligomers into the PM film, and their subsequent condensation and retention as nano-thin inorganic lamellae

within the composite mesostructure after drying. Our results indicate that the intercalated nanocomposites prepared from preformed PM films have a higher degree of ordering than those produced by co-assembly.

Materials, sample preparation and experimental methods

In situ X-ray surface scattering studies of the PM films were carried out at the XMaS UK CRG beamline (BM 28) at the European Synchrotron Radiation Facility (ESRF) in Grenoble, France. The monochromatic X-ray beam had an energy of 10 keV with a corresponding wavelength $\lambda = 1.24$ Å. The beam size on the sample position was 300 μm × 300 μm (height × width). The incident angle θ_i was varied in the range 0.06–2° for each of the measurements, corresponding to a momentum transfer $Q = 4\pi \sin \theta_i/\lambda$ range of 0.011–0.345 Å^{-1}. The surface scattering data were collected by X-ray reflectivity (XRR),[19–21,24,25] using an avalanche photodiode detector in the specular reflection plane, but at reflection angles θ_f with a small offset $\Delta\theta = 0.06°$ ($\theta_f = \theta_i \pm \Delta\theta$) to the incident angle (θ_i) to minimise the contribution from the silicon substrate. PM samples on solid silicon substrates were mounted inside a small chamber enclosed with Kapton films, which allowed a constant flow of helium (He) during the measurements to reduce background scattering and sample damage. Each sample was assessed for visible damage after alignment. Beam damage was checked by taking measurements on several regions of the film, moving the sample perpendicular to the incident beam.

Aminopropyl silicic acid (APS) solutions were prepared as detailed previously.[17] Briefly, 5 mL of 3-aminopropyltriethoxysilane was added to 20 mL of 0.5 M HCl in a 50 mL round bottomed flask. The flask contents were rotary evaporated in a water bath at 45 °C for 15–20 minutes until the generated ethanol had been removed. The APS concentration in the solution was determined by drying and condensing small aliquots in pre-weighed vials. Solutions were diluted with distilled water to the desired concentrations.

Aqueous sols of polycationic AMP organoclay oligomers were prepared at room temperature by drop-wise addition of 3-aminopropyltriethoxysilane (1.3 mL, 5.85 mmol) to an ethanolic solution of magnesium chloride (0.84 g, 3.62 mmol) in ethanol (20 g).[22,23] A white slurry was obtained after 5 min which was stirred overnight and the precipitate isolated by centrifugation, washed with ethanol (50 mL) and dried at 40 °C. Exfoliation of the clay was undertaken by dispersing 10 mg of the dried clay in distilled water (10 mL) followed by ultrasonication for 5 min. The resulting cloudy dispersion, with a measured zeta potential of +12 mV at pH 8.5, was passed through a Sephadex G-25/75 column (Aldrich), and the clear eluate of polycationic organoclay clusters collected.

The pristine PM film (*i.e.* without guest materials) was prepared by placing a 60 μL droplet of an aqueous PM dispersion (5.5 mg mL^{-1}) to the centre of a hydrophilic silicon wafer (1 × 2 cm). The droplet was allowed to dry slowly at room temperature and 60–70% RH, resulting in a film approximately

5448 | *J. Mater. Chem. C*, 2014, **2**, 5447–5452

This journal is © The Royal Society of Chemistry 2014

circular in shape, 4–5 mm in diameter and 5–10 μm in thickness.

APS or AMP intercalation into preformed PM films was undertaken by adding 60 μL of a 5.5 mg mL^{-1} 3-aminopropyl silicic acid or organoclay solution to a preformed PM film mounted on a silicon wafer using a volumetric pipette. For *in situ* XRR studies, the PM film-containing silicon substrate was first aligned in the X-ray beam, and then a droplet of APS or AMP solution added on top of the PM film. XRR scans were then taken at different time intervals as the solution was allowed to dry at ambient RH (45–55%), and the measurements repeated at different positions on the film. Alternatively, composite films were prepared by a co-assembly procedure in which an aqueous solution of APS or AMP was mixed with an aqueous dispersion of PM sheets for ~1 minute prior to deposition of the mixture on a bare silicon wafer that was pre-aligned in the X-ray beam. Co-assembly was undertaken by adding 60 μL of 5.5 mg mL^{-1} PM in water to 60 μL of 5.5 mg mL^{-1} aqueous APS or AMP solution in a small centrifuge tube. This mixture was drawn into a volumetric pipette and then deposited onto the silicon wafer.

Results and discussion

Formation of interstitial hydration layers due to wetting of PM films

The XRR profile of the pre-dried pristine PM film control sample displayed two prominent Bragg peaks at $Q_1 = 0.134$ Å^{-1} and $Q_2 = 0.265$ Å^{-1} (Fig. 1a). The ratio of $Q_1/Q_2 \approx 1:2$ indicated that these two peaks corresponded to the (001) ($n = 1$) and (002) ($n = 2$) diffractions respectively, as a result of a lamellar structure
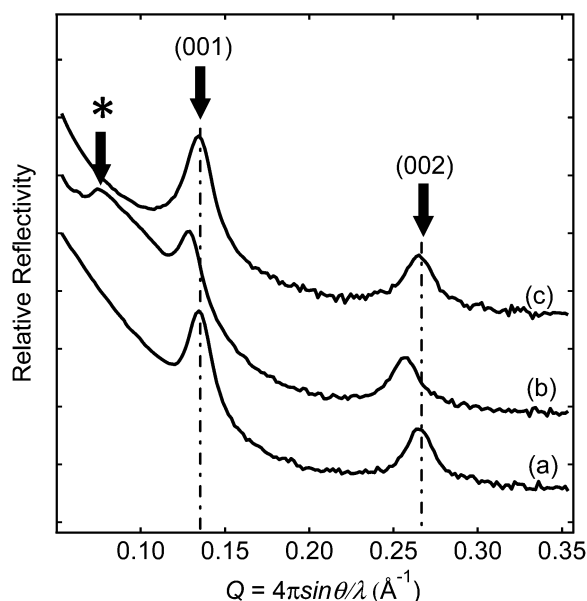
with an average d-spacing of $d = 2n\pi/Q_n = 4.70$ nm in the PM film, with the lamellar plane approximately parallel to the Si substrate. This was consistent with the repeat distance for PM films observed at minimum hydration, and the expected thickness for a single purple membrane bilayer without water present interstitially or absorbed from the atmosphere during the experiment.[6] From fitting the Bragg peaks with a Gaussian function, the coherence length, L, of the ordered domains in the film was calculated using the Scherrer equation, $L = 2\pi K/\Delta Q$, where ΔQ is the full width at half maximum (FWHM) of the peak and K is a shape factor of order unity.[24–26] Such an analysis gave a value of L of ~71 nm for the dry PM control film, which corresponded to an ordered domain of approximately 14 lipid bilayers (average number of bilayers, $m = L/d \sim 14$). The calculated values of d, L and m for all the PM films studied are listed in Table 1.

To examine PM hydration, the XRR profile of a control PM film was recorded, and then a 60 μL water droplet added on top of the film, which subsequently spread and wetted the film. The wetted PM film was subject to a constant flow of He for 15 minutes to remove residual surface water, and then the He flow was stopped and XRR curves were collected as the film gradually dehydrated at an RH of ~50%. After 15 min of drying, the (001) and (002) Bragg peaks were shifted to slightly smaller Q values ($Q_1 = 0.128$ Å^{-1} and $Q_2 = 0.256$ Å^{-1} respectively; average d-spacing = 4.90 nm) (Fig. 1b), indicating a small swelling of ~0.2 nm as compared to the dry control film. Significantly, a broad peak at $Q = 0.077$ Å^{-1} was also observed, corresponding to a d-spacing of 8.20 nm. This peak was attributed to an interstitial water layer of around 3.5 nm in thickness.

The coexistence of the three Bragg peaks suggested that the partially dried PM film was not homogeneously hydrated but consisted of a mixture of extensively hydrated lamellar domains along with regions that remained essentially dehydrated. After further drying under He flow, the PM film returned to a completely dehydrated state and the XRR curve showed that Bragg reflections re-emerged at Q values ($Q_1 = 0.134$ Å^{-1} and $Q_2 = 0.268$ Å^{-1}; average d-spacing = 4.70 nm) (Fig. 1c), which were identical to those for the initial sample of the dried PM film.

Fig. 1 XRR curves for (a) a fully dried pristine PM film on a silicon substrate; (b) the same film after the addition of water to the surface and subsequent drying for 15 min; and (c) after complete dehydration. The major diffraction peaks are marked by arrows and denoted by dot-dashed lines. Asterisk (*) shows the (001) reflection for the swollen lamellar phase.

Table 1 Structural information for purple membrane (PM) films treated with solutions of different guest molecules. Composite films were prepared from preformed PM films or *via* host–guest co-assembly. (* = peak indicated by * in Fig. 1)

Samples	Lamellar layer thickness, d (nm)	Coherent length, L (nm)	Average number of layers, m
PM control film	4.70	66.7	14
Hydrated PM film	4.90, 8.20*	54.6, 14.1*	11, 2*
Dehydrated PM film	4.70	60.5	13
PM prior addition of APS	4.70	60.0	13
PM/APS (after 12 minutes)	—	—	—
PM/APS (fully dried)	5.40	51.1	10
PM/APS (co-assembly)	6.24	23.2	4
PM/organoclay (preformed)	5.50	34.3	6
PM/organoclay (co-assembly)	5.23	22.4	4

This journal is © The Royal Society of Chemistry 2014

J. Mater. Chem. C, 2014, **2**, 5447–5452 | **5449**

Mechanism of aminopropyl silicic acid (APS) intercalation into PM films

A droplet of APS was added to a dried PM film after obtaining the XRR profile of the preformed mesolamellar structure ($Q_1 = 0.134$ Å^{-1} and $Q_2 = 0.268$ Å^{-1}; d-spacing ~ 4.70 nm, $L \sim 60$ nm, $m \sim 13$; Fig. 2a), and the surface X-ray scattering curve of the wet sample re-recorded after 12 minutes. The profile showed a complete absence of the characteristic Bragg peaks (Fig. 2b), suggesting that the PM stacks were delaminated or extensively disordered at a local level in the presence of aqueous APS. The wetted film was then dried under a flow of He for 3 minutes and the XRR scan collected. Bragg peaks corresponding to (001) and (002) planes at $Q_1 = 0.116$ Å^{-1} and $Q_2 = 0.233$ Å^{-1} at an expanded d spacing of 5.40 nm reappeared (Fig. 2c). Re-emergence of the Bragg reflections indicated that the wetted film was reconstructed into a lamellar composite on loss of bulk water. However, the coherence length L was decreased to a value between 51.1 nm (10 layers) as compared to the native PM film, suggesting a more disordered mesostructure. This was consistent with the intercalation of a 0.75 nm-thick sheet of organosilica between the membrane bilayers.

The complete loss of structural order upon wetting (Fig. 2b) suggested that the lamellar structure was largely dissociated prior to reassembly upon drying and intercalation. As a consequence, the possibility that intercalation of APS takes place *via* an exchange mechanism in which the guest molecules permeate a well-ordered matrix of PM sheets seems highly unlikely. In contrast, the presence of a 3.5 nm-thick hydration interstitial layer in the partially dried PM films (*cf.* Fig. 1b), suggests that this transient phase could provide the mechanism for spontaneous sequestration of APS molecules. However, upon deposition of the APS containing droplet, the PM film structure was much more disordered, evident from the absence of the absence of the Bragg peaks in Fig. 2b. APS may subsequently become entrapped in the form of a continuous organosilica matrix due to the onset of condensation reactions associated with further dehydration, leading to reformation of ordered lamellar structure and re-emergence of the Bragg peaks in Fig. 2c. The time for each XRR alignment and scan for such *in situ* measurements was ~ 2 h. As such, it is also possible that we did not have the time resolution to fully capture the detail of the time evolution in the structural change during the intercalation process. However, it is clear that the aqueous environment and its lubricant-like role is essential to facilitating intercalation.

This mechanism was further tested by examining the structure of composite films prepared *via* dehydration-induced co-assembly from an aqueous mixture of PM sheets and APS. The XRR curve for the co-assembled film showed a broad reflection peak at $Q = 0.101$ Å^{-1} ($d = 6.24$ nm) attributed to the (001) plane (Fig. 2d). The estimated coherence length from this was calculated to be $L \sim 23$ nm ($m \sim 4$). No (002) reflection was observed, indicating that the composites produced by co-assembly were more disordered than those prepared by intercalation within a preformed PM film. Given that the co-assembled films also showed an increase in the interlayer spacing of approximately 1 nm compared with nanocomposites produced from preformed PM films, the increased organosilica content and structural disorder suggested that mixing the components in suspension prior to film formation increased the level of host–guest pre-organization. A schematic representation of the proposed intercalation mechanism is shown in Fig. 3.
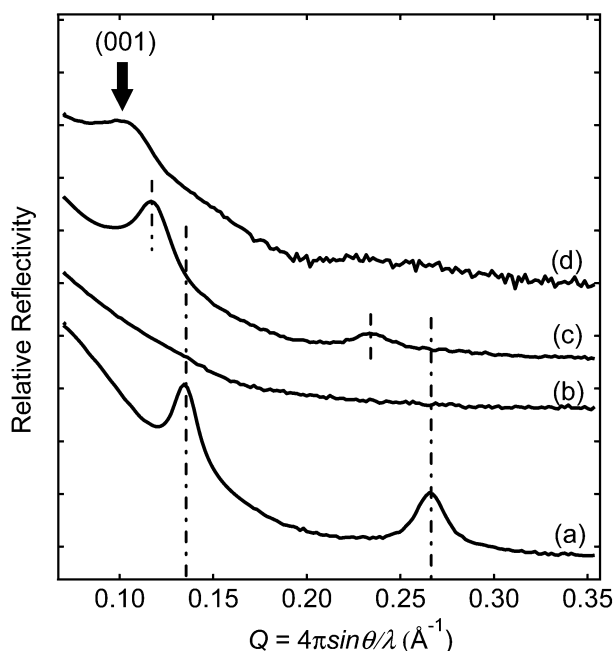

Fig. 2 XRR curves for (a) a control PM film prior to the addition of APS solution; (b) the preformed PM film 12 minutes after wetting with APS solution; (c) the preformed PM film exposed to APS solution after being allowed to dry completely; and (d) a PM/organosilane film formed *via* co-assembly using identical amounts of PM and APS solution as for (b). Dot-dashed lines indicate the major reflections. All samples were formed on a silicon substrate.

Intercalation of organoclay clusters into PM films

As a comparison to the APS system, the intercalation of poly-cationic AMP organoclay clusters *ca.* 1.6 nm in size[16] with PM sheets to produce structured nanocomposites was investigated by XRR. While *in situ* condensation of entrapped APS resulted in the formation of an intercalated organosilica layer that conforms to the size of the interstitial water layer, the organoclay oligomers assemble as preformed units while confined between the PM layers to produce an ordered lamellar structure. In this regard, electrostatic interactions between the poly-cationic clusters and negatively charged surface of PM sheets could provide a feasible mechanism for sequestering high concentrations of the AMP clusters within the stacked meso-lamellar structure.

An XRR scan of an AMP/PM composite film prepared by addition of an aqueous droplet of AMP to a preformed air-dried PM film displayed very broad (001) and (002) reflections at $Q_1 \sim 0.115$ Å^{-1} ($d \sim 5.50$ nm) and $Q_2 \sim 0.231$ Å^{-1}, respectively (Fig. 4a). The coherence length L calculated from the (001) peak was 34.3 nm ($m = 6$), which was almost half that for the PM/organosilane composite films ($m = 10$) produced under similar
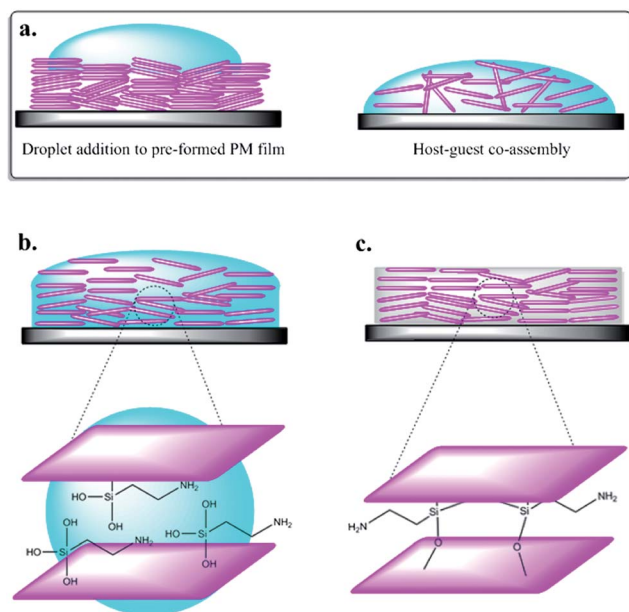
5450 | *J. Mater. Chem. C*, 2014, **2**, 5447–5452

This journal is © The Royal Society of Chemistry 2014

Fig. 3 (a) A schematic showing the two methods of composite film preparation: a droplet containing APS solution added to a preformed PM film and host–guest co-assembly from mixing the components together prior to drying. (b) The transient phase of intercalation in which the PM lamellar structure becomes disordered and swollen with the solution. (c) Upon complete dehydration, the APS is condensed into a solid organosilane interstitially between PM layers.

conditions. The XRR profile of an AMP/PM composite film prepared by co-assembly of the constituents also displayed one very broad (001) peak centred at $Q \sim 0.12 \text{ Å}^{-1}$ ($d \sim 5.23$ nm, $L = 22.4$ nm, $m \sim 4$) (Fig. 4b), but no (002) reflection was observed.
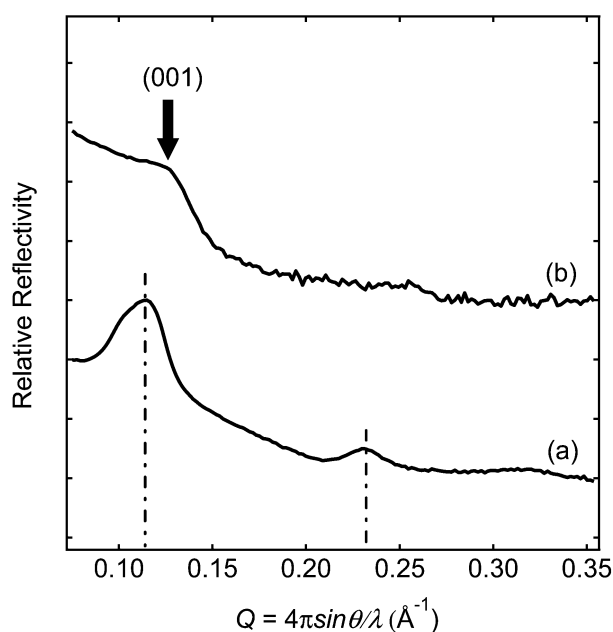

Fig. 4 XRR plots for a PM/AMP composite film formed by (a) addition of a solution of organoclay clusters to a preformed PM film and then allowed to dry completely; and (b) mixing a PM dispersion in water with an organoclay solution, followed by drying to induce co-assembly.

Although mixing the PM sheets and organoclay oligomers produces a uniform mixture prior to dehydration and co-assembly, the increased level of interaction between the components when dispersed together in bulk solution, could result in complexation and formation of hybrid sheets that are less structurally homogeneous, and hence less likely to stack in an ordered configuration. Another possibility is that complexation between the components disrupts the formation of an interstitial water layer during the assembly process, which in turn results in poor ordering.

Overall, the results indicated that intercalation of the organoclay clusters produced a less ordered mesolamellar composite compared with samples produced in the presence of APS. The *in situ* reactivity of the APS molecules when dehydrated allowed the condensed phase to conform to the lamellar environment to a greater degree than the solid clay layers, resulting in longer range ordering observed. In both systems, co-assembly of the constituents increased the level of disorder in the hybrid nanocomposites.

Summary and concluding remarks

Our surface scattering results show that hydration layers of $\sim$3.5 nm formed in the inter-lamellar space when PM films were exposed to water. We suggest that this interstitial hydration layer plays a critical role in mediating intercalation of guest materials delivered *via* an aqueous medium. To elucidate the intercalation mechanism, we used *in situ* XRR measurements on lamellar-structured composite films prepared from preformed PM films or *via* host–guest co-assembly. The results showed that loss of the preformed PM lamellar structure occurs upon addition of a droplet of aqueous APS solution, and that a new lamellar phase with a larger interlayer spacing attributed to intercalation of APS or AMP is produced upon drying. We suggest that this assembly mechanism facilitates the infiltration of the guest molecules or clusters, as diffusion into the highly hydrated disordered intermediate structure is facile. Moreover, formation of an ordered hydration layer during partial drying enables the guest molecules and clusters to be sequestered within the incipient lamellar phase. Subsequent solidification of the intercalated precursors *via* drying-induced sol–gel condensation reactions then provides a mechanism for retention of the guest species within the layered nanocomposite. In contrast, co-assembly of the host and guest components from a mixed aqueous dispersion produces intercalated composites but with a lower degree of structural order.

Understanding the intercalation mechanism should offer important insights for the synthesis of PM-based composite lamellar films with a range of potential guest inorganic or polymeric materials. The presence of a guest material within the PM layers tends to reduce the extent of long range order (coherence length) in the composite films, which could compromise functionality. Thus, mechanistic insights are required to inform how these materials should be optimised in terms of guest loading capacity and the concomitant effects on the structural organization of the PM composite films. Such

considerations will be of particular importance for PM films comprising confined ensembles of reactive guest species.

We note that grazing incidence X-ray scattering (GIXS) on our system can yield complementary in-plane structural information,[21,27–29] and our future work will aim to make use of GIXS to further explore the proposed mechanism.

Acknowledgements

Notes and references

1 D. Oesterhelt and W. Stoeckenius, *Nature*, 1971, **233**, 149–152.

2 A. Popp, M. Wolperdinger, N. Hampp, C. Bräuchle and D. Oesterhelt, *Biophys. J.*, 1993, **65**, 1449–1459.

3 B. Yao, Z. Ren, N. Menke, Y. Wang, Y. Zheng, M. Lei, G. Chen and N. Hampp, *Appl. Opt.*, 2005, **44**, 7344–7348.

4 W. Kühlbrandt, *Nature*, 2000, **406**, 569–570.

5 J. K. Lanyi, *Mol. Membr. Biol.*, 2004, **21**, 143–150.

6 S. Grudinin, G. Büldt, V. Gordeliy and A. Baumgaertner, *Biophys. J.*, 2005, **88**, 3252–3261.

7 L. Frish, N. Friedman, M. Sheves and Y. Cohen, *Biopolymers*, 2004, **75**, 46–59.

8 N. A. Dencher, H. J. Sass and G. Büldt, *Biochim. Biophys. Acta*, 2000, **1460**, 192–203.

9 G. Zaccai, *Biophys. Chem.*, 2000, **86**, 249–257.

10 M. Saab, E. Estephan, T. Cloitre, R. Legros, F. J. G. Cuisinier, L. Zimányi and C. Gergely, *Langmuir*, 2009, **25**, 5159–5167.

11 R. P. Baumann, A. P. Busch, B. Heidel and N. Hampp, *J. Phys. Chem. B*, 2012, **116**, 4134–4140.

12 A. M. Collins, N. H. Mohd Kaus, F. Speranza, W. H. Briscoe, D. Rhinow, N. Hampp and S. Mann, *J. Mater. Chem.*, 2010, **20**, 9037–9041.

13 K. Wood, M. Plazanet, F. Gabel, B. Kessler, D. Oesterhelt, G. Zaccai and M. Weik, *Eur. Biophys. J.*, 2008, **37**, 619–626.

14 S. A. Verclas, P. B. Howes, K. Kjaer, A. Wurlitzer, M. Weygand, G. Büldt, N. A. Dencher and M. Lösche, *J. Mol. Biol.*, 1999, **287**, 837–843.

15 Y. Shen, C. Safinya and K. Liang, *Nature*, 1993, **366**, 48–50.

16 K. M. Bromley, A. J. Patil, A. M. Seddon, P. Booth and S. Mann, *Adv. Mater.*, 2007, **19**, 2433–2438.

17 A. M. Collins, D. Rhinow, N. Hampp and S. Mann, *Biomacromolecules*, 2009, **10**, 2767–2771.

18 S. C. Holmström, A. J. Patil, M. Butler and S. Mann, *J. Mater. Chem.*, 2007, **17**, 3894–3900.

19 F. Speranza, G. A. Pilkington, T. G. Dane, P. T. Cresswell, P. Li, R. M. J. Jacobs, T. Arnold, L. Bouchenoire, R. K. Thomas and W. H. Briscoe, *Soft Matter*, 2013, **9**, 7028–7041.

20 W. H. Briscoe, F. Speranza, P. Li, O. Konovalov, L. Bouchenoire, J. van Stam, J. Klein, R. M. J. Jacobs and R. K. Thomas, *Soft Matter*, 2012, **8**, 5055–5068.

21 L. Cristofolini, *Curr. Opin. Colloid Interface Sci.*, 2014, DOI: 10.1016/j.bbr.2011.03.031.

22 A. J. Patil, E. Muthusamy and S. Mann, *Angew. Chem., Int. Ed.*, 2004, **43**, 4928–4933.

23 A. J. Patil, E. Muthusamy and S. Mann, *J. Mater. Chem.*, 2005, **15**, 3838–3843.

24 T. G. Dane, P. T. Cresswell, O. Bikondoa, G. E. Newby, T. Arnold, C. F. J. Faul and W. H. Briscoe, *Soft Matter*, 2012, **8**, 2824–2832.

25 J. M. Bulpett, A. M. Collins, N. H. M. Kaus, P. T. Cresswell, O. Bikondoa, D. Walsh, S. Mann, S. A. Davis and W. H. Briscoe, *J. Mater. Chem.*, 2012, **22**, 15635–15643.

26 A. Patterson, *Phys. Rev.*, 1939, **56**, 978–982.

27 P. Kohn, Z. Rong, K. Scherer and A. Sepe, *Macromolecules*, 2013, **46**, 4002–4013.

28 T. G. Dane, P. T. Cresswell, G. A. Pilkington, S. Lilliu, J. E. Macdonald, S. W. Prescott, O. Bikondoa, C. F. J. Faul and W. H. Briscoe, *Soft Matter*, 2013, **9**, 10501.

29 T. M. Yeh, Z. Wang, D. Mahajan, B. S. Hsiao and B. Chu, *J. Mater. Chem. A*, 2013, **1**, 12998–13003.